

New Multigroup Transport Equations Derived via Homogeneity and Isotropy Restoration (HIRE) Theory

Nam Zin Cho
`nzcho@kaist.ac.kr`



*Presented in the Plenary Session at
PHYTRA5 in Xian, China (online)
May 10-11, 2021*

Table of Contents

1. Introduction

- Limitations of Conventional Multigroup Transport Equations

2. Methodology of New Multigroup (**Few Group**) Transport Equations

- Homogeneity and Isotropy Restoration (**HIRE**) Theory
- Partial Current Discontinuity Factor (**PCDF**) Iteration
- JFNK Method with Exponential Transformation

3. Numerical Results

- Test Problem 1 : 1 pin-cell size (reflective BC)
- Test Problem 2 : 1 pin-cell size (albedo BC)
- Test Problem 3 : 4 pin-cell size (reflective BC)
- Test Problem 4 : 16 pin-cell size (**baffle effect**)
- Test Problem 5 : 1 pin-cell size (**rim effect** in depletion)

4. Summary and Concluding Remarks

5. References

1. Introduction (1/3)

□ Continuous-energy neutron transport equation is rigorously derived as:

$$\vec{\Omega} \cdot \nabla \varphi(\vec{r}, E, \vec{\Omega}) + \sigma_t(\vec{r}, E) \varphi(\vec{r}, E, \vec{\Omega}) = \int d\Omega' \int dE' \sigma_s(\vec{r}, E' \rightarrow E, \vec{\Omega}' \rightarrow \vec{\Omega}) \varphi(\vec{r}, E', \vec{\Omega}') + \frac{\chi(E)}{k_{eff}} \int d\Omega' \int dE' \nu \sigma_f(\vec{r}, E') \varphi(\vec{r}, E', \vec{\Omega}'). \quad (1)$$

□ To obtain corresponding multigroup transport equations, Eq. (1) is integrated over an energy interval $E_g \leq E \leq E_{g-1}$ leading to:

$$\vec{\Omega} \cdot \nabla \varphi_g(\vec{r}, \vec{\Omega}) + \sigma_{t,g}(\vec{r}, \vec{\Omega}) \varphi_g(\vec{r}, \vec{\Omega}) = \sum_{g'=1}^G \int d\Omega' \sigma_{s,gg'}(\vec{r}, \vec{\Omega}' \rightarrow \vec{\Omega}) \varphi_{g'}(\vec{r}, \vec{\Omega}') + \frac{\chi_g}{k_{eff}} \sum_{g'=1}^G \nu \sigma_{f,g'}(\vec{r}) \phi_{g'}(\vec{r}), \quad (2)$$

where the standard notations are used.

1. Introduction (2/3)

- Note that the group total cross section in Eq. (2) becomes angle-dependent and space-dependent as:

$$\sigma_{t,g}(\vec{r}, \vec{\Omega}) = \frac{\int_{E_g}^{E_{g-1}} dE \sigma_t(\vec{r}, E) \varphi(\vec{r}, E, \vec{\Omega})}{\int_{E_g}^{E_{g-1}} dE \varphi(\vec{r}, E, \vec{\Omega})}. \quad (3)$$

- Previous studies on angle-dependency of the group total cross section

- Removal of angle-dependency
 - Consistent P approximation
 - Extended (BHS) transport approximation: outflow/inflow approximations
- Angle-dependency is expanded in Legendre functions and retained in LHS.
 - Anisotropic media approach
- Angle-dependent portion is moved to RHS and expanded in spherical harmonics and added to the scattering term.
 - Generalized energy condensation (GEC) scheme

1. Introduction (3/3)

□ Homogeneity and Isotropy Restoration (HIRE) Theory in this presentation:

- **Homogeneity** in material region
- Angle-independence in total XS
- Preservation of **region-wise reaction rate**

are achieved in the derivation of multigroup transport equations by the device of **partial current discontinuity factor** (PCDF).

2. Methodology: Problems of Multigroup XS (1/7)

□ On reaction terms in Eq. (2), we perform, over V_m of material region m ,

$$\sigma_{t,g}(\vec{r}, \vec{\Omega}) = \frac{\int_{E_g}^{E_{g-1}} dE \sigma_t(\vec{r}, E) \varphi(\vec{r}, E, \vec{\Omega})}{\int_{E_g}^{E_{g-1}} dE \varphi(\vec{r}, E, \vec{\Omega})}, \quad \text{blue arrow} \quad (3)$$

$$\sigma_{t,g}^m = \frac{\int_{\vec{r} \in V_m} dV \int d\Omega \int_{E_g}^{E_{g-1}} dE \sigma_t(\vec{r}, E) \varphi(\vec{r}, E, \vec{\Omega})}{\int_{\vec{r} \in V_m} dV \int d\Omega \int_{E_g}^{E_{g-1}} dE \varphi(\vec{r}, E, \vec{\Omega})}, \quad (3a)$$

$$\sigma_{s,gg'}(\vec{r}, \vec{\Omega}' \rightarrow \vec{\Omega}) = \frac{\int_{E_g}^{E_{g-1}} dE \int d\Omega' \int_{E_{g'}}^{E_{g'-1}} dE' \sigma_s(\vec{r}, E' \rightarrow E, \vec{\Omega}' \rightarrow \vec{\Omega}) \varphi(\vec{r}, E', \vec{\Omega}')}{\int_{E_{g'}}^{E_{g'-1}} dE' \varphi(\vec{r}, E', \vec{\Omega}')}, \quad \text{blue arrow} \quad (4)$$

$$\sigma_{s0,gg'}^m = \frac{\int_{\vec{r} \in V_m} dV \int d\Omega \int_{E_g}^{E_{g-1}} dE \int d\Omega' \int_{E_{g'}}^{E_{g'-1}} dE' \sigma_s(\vec{r}, E' \rightarrow E, \vec{\Omega}' \rightarrow \vec{\Omega}) \varphi(\vec{r}, E', \vec{\Omega}')}{\int_{\vec{r} \in V_m} dV \int d\Omega \int d\Omega' \int_{E_{g'}}^{E_{g'-1}} dE' \varphi(\vec{r}, E', \vec{\Omega}')}, \quad (4a)$$

2. Methodology: Problems of Multigroup XS (2/7)

$$\nu\sigma_{f,g'}(\vec{r}) = \frac{\int d\Omega' \int_{E_{g'}}^{E_{g'-1}} dE' \nu\sigma_f(\vec{r}, E') \varphi(\vec{r}, E', \vec{\Omega}')}{\int d\Omega' \int_{E_{g'}}^{E_{g'-1}} dE' \varphi(\vec{r}, E', \vec{\Omega}')} \quad \rightarrow \quad (5)$$

$$\nu\sigma_{f,g'}^m = \frac{\int_{\vec{r} \in V_m} dV \int d\Omega \int d\Omega' \int_{E_{g'}}^{E_{g'-1}} dE' \nu\sigma_f(\vec{r}, E') \varphi(\vec{r}, E', \vec{\Omega}')}{\int_{\vec{r} \in V_m} dV \int d\Omega \int d\Omega' \int_{E_{g'}}^{E_{g'-1}} dE' \varphi(\vec{r}, E', \vec{\Omega}')}, \quad (5a)$$

$$\chi_g^m = \frac{\int_{\vec{r} \in V_m} dV \int d\Omega \int_{E_g}^{E_{g-1}} dE \int d\Omega' \sum_{g'=1}^G \int_{E_{g'}}^{E_{g'-1}} dE' \chi(E) \nu\sigma_f(\vec{r}, E') \varphi(\vec{r}, E', \vec{\Omega}')}{\int_{\vec{r} \in V_m} dV \int d\Omega \int d\Omega' \sum_{g'=1}^G \int_{E_{g'}}^{E_{g'-1}} dE' \nu\sigma_f(\vec{r}, E') \varphi(\vec{r}, E', \vec{\Omega}')}. \quad (6a)$$

- The above multigroup constants are obtained by tallies from the continuous-energy Monte Carlo calculation on a **unit problem** with albedo boundary condition α .

2. Methodology: HIRE Theory (3/7)

□ Multigroup Transport Equations

- Eq. (2) becomes, after averaging over each material region and integrating over angle,

$$\frac{1}{V_m} \int_{\partial V_m} dA \vec{n} \cdot \vec{J}(\vec{r}) + \sigma_{t,g}^m \phi_g^m = \sum_{g'=1}^G \sigma_{s0gg'}^m \phi_{g'}^m + \frac{\chi_g^m}{k_{eff}} \sum_{g'=1}^G \nu \sigma_{f,g'}^m \phi_{g'}^m, \quad (7)$$

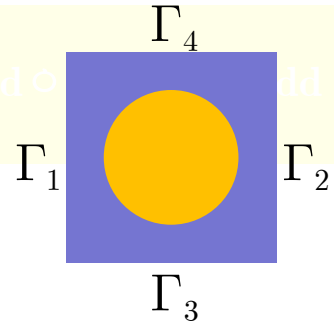
where $\vec{J}_g(\vec{r}) = \int d\Omega \vec{\Omega} \varphi(\vec{r}, \vec{\Omega})$, $\phi_g^m = \frac{1}{V_m} \int_{\vec{r} \in V_m} dV \phi_g(\vec{r})$.

- Eq. (2) is then recast in the following multigroup equations with cross sections of Eqs. (3a)–(6a):

$$\vec{\Omega} \cdot \nabla \varphi_g(\vec{r}, \vec{\Omega}) + \sigma_{t,g}^m \varphi_g(\vec{r}, \vec{\Omega}) = \sum_{g'=1}^G \sigma_{s0gg'}^m \phi_{g'}(\vec{r}) + \frac{\chi_g^m}{k_{eff}} \sum_{g'=1}^G \nu \sigma_{f,g'}^m \phi_{g'}(\vec{r}), \quad (8)$$

with albedo boundary condition $\varphi_g(\vec{r}, \vec{\Omega}') = \alpha_k \varphi_g(\vec{r}, \vec{\Omega})$, $k = 1$ to 4 .

- Eq. (8) is the multigroup transport equations, derived in this paper.
- Only σ_{s0} term remains : a byproduct
- Eigenvalue** and **material region-wise flux distributions**, as such obtained with the usual continuity conditions, will show discrepancies compared to those from the continuous-energy calculation. \Leftrightarrow **PCDF**



2. Methodology: HIRE Theory (4/7)

□ Partial Current Discontinuity Factor (PCDF)

- To preserve the reference neutron leakages, PCDF is introduced to each outgoing and incoming current with respect to material region surface k (Γ_k , $k=1$ to 8) as:

$$f_{g,k}^+ \varphi_g(\vec{r}_k, \vec{\Omega}) \quad \text{for } \vec{\Omega} \cdot \vec{n}_k > 0, \quad (9a)$$

$$f_{g,k}^- \varphi_g(\vec{r}_k, \vec{\Omega}) \quad \text{for } \vec{\Omega} \cdot \vec{n}_k < 0, \quad (9b)$$

where $f_{g,k}^\pm$ are initially guessed and updated by PCDF iterations.

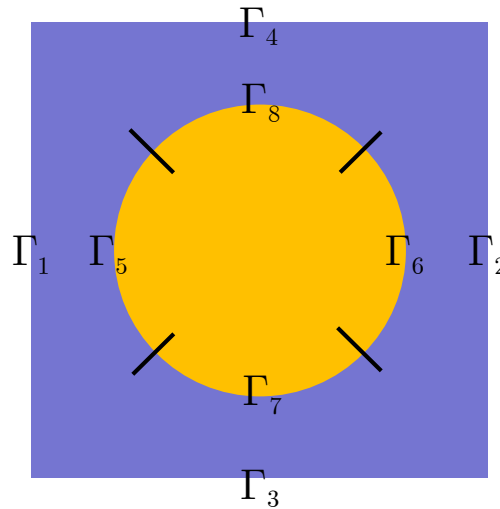


Fig. 1. Surface divisions for PCDFs.

2. Methodology: HIRE Theory (5/7)

□ Update of PCDFs

- Partial currents obtained from the multigroup transport solution:

$$J_{g,k}^+ = \int_{\vec{r} \in \Gamma_k} dA \int_{\vec{\Omega} \cdot \vec{n}_k > 0} d\Omega |\vec{n}_k \cdot \vec{\Omega}| \varphi_g(\vec{r}, \vec{\Omega}), \quad (10a)$$

$$J_{g,k}^- = \int_{\vec{r} \in \Gamma_k} dA \int_{\vec{\Omega} \cdot \vec{n}_k < 0} d\Omega |\vec{n}_k \cdot \vec{\Omega}| \varphi_g(\vec{r}, \vec{\Omega}). \quad (10b)$$

- Discontinuity in partial currents:

$$\tilde{J}_{g,k}^- = f_{g,k}^- J_{g,k}^-, \quad (11a)$$

$$\tilde{J}_{g,k}^+ = f_{g,k}^+ J_{g,k}^+. \quad (11b)$$

- Conditions on the updated PCDFs:

$$J_{g,k}^{ref} = J_{g,k}^+ - \tilde{J}_{g,k}^- = J_{g,k}^+ - f_{g,k}^- J_{g,k}^- \Leftrightarrow f_{g,k}^- = \frac{J_{g,k}^+ - J_{g,k}^{ref}}{J_{g,k}^-}, \quad (12a)$$

$$J_{g,k}^{ref} = \tilde{J}_{g,k}^+ - J_{g,k}^- = f_{g,k}^+ J_{g,k}^+ - J_{g,k}^- \Leftrightarrow f_{g,k}^+ = \frac{J_{g,k}^- + J_{g,k}^{ref}}{J_{g,k}^+}. \quad (12b)$$

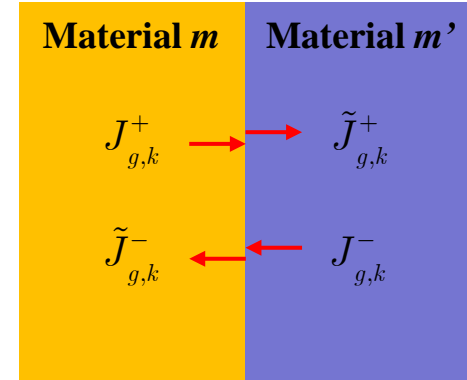


Fig. 2. Leakage corrections based on PCDFs at interface k .

Reference surface net current $J_{g,k}^{ref}$ from the continuous-energy MC calculation

2. Methodology: HIRE Theory (6/7)

❑ PCDF iteration scheme

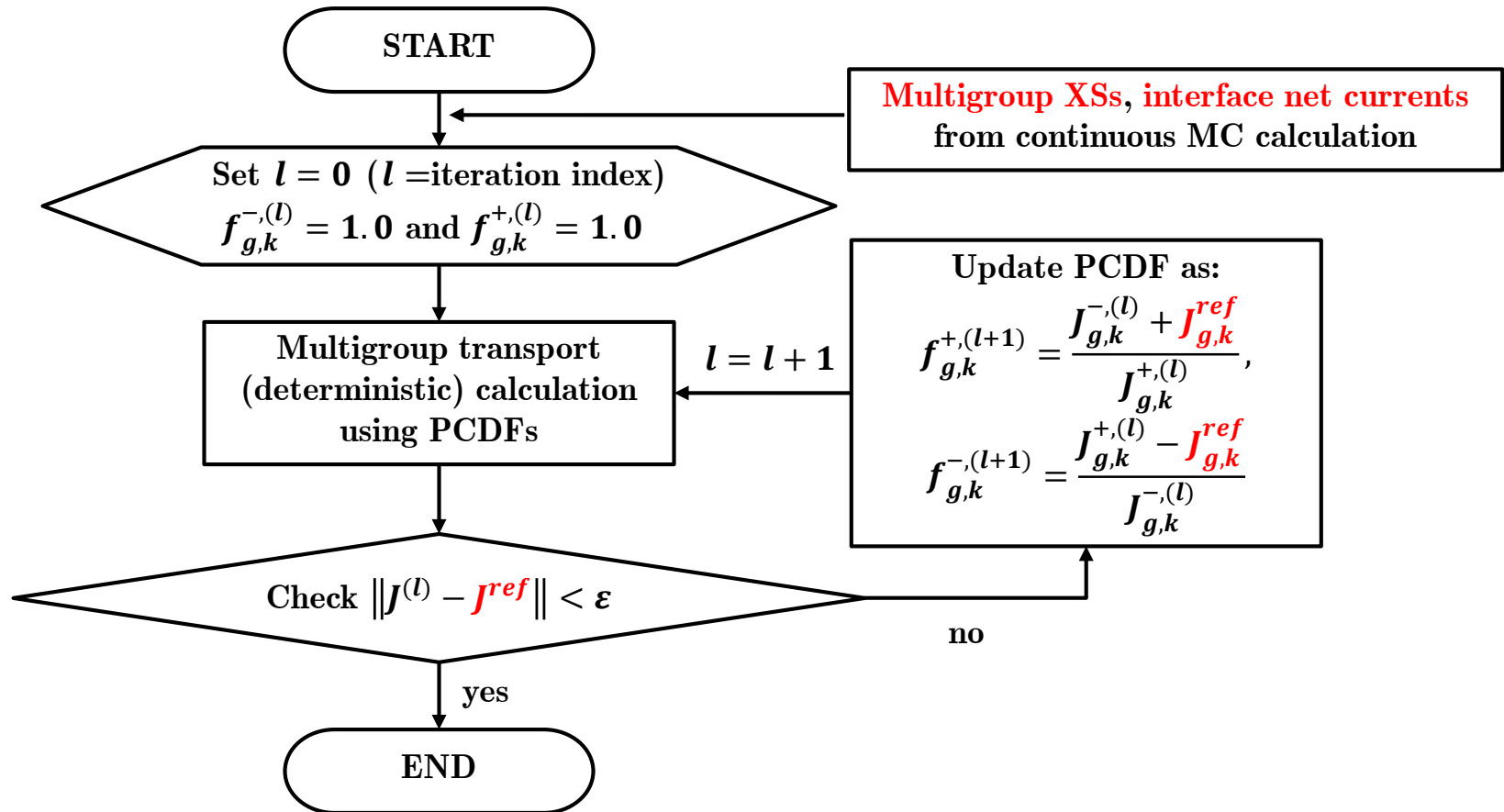


Fig. 3. Flow Chart of PCDF Iteration.

2. Methodology: HIRE Theory (7/7)

□ JFNK Method with Exponential Transformation

$$1) \quad \vec{F}(\vec{f}) = \left(F_{g,k}^{\pm}(\vec{f}) \right)_{g=1..G, k=1..8} = 0,$$

where

$$F_{g,k}^{\pm}(\vec{f}) = \frac{J_{g,k}^{\mp}(\vec{f}) + J_{g,k}^{ref}}{J_{g,k}^{\pm}(\vec{f})} - f_{g,k},$$

$$\vec{f} = \left(f_{g,k}^{\pm} \right)_{g=1..G, k=1..8}.$$

$$2) \quad \text{Since } \vec{f} > 0,$$

$$\vec{G}(\vec{x}) \equiv \vec{F}(\exp(\vec{x})) = 0.$$

Then, the PCDFs become $\exp(\vec{x})$.

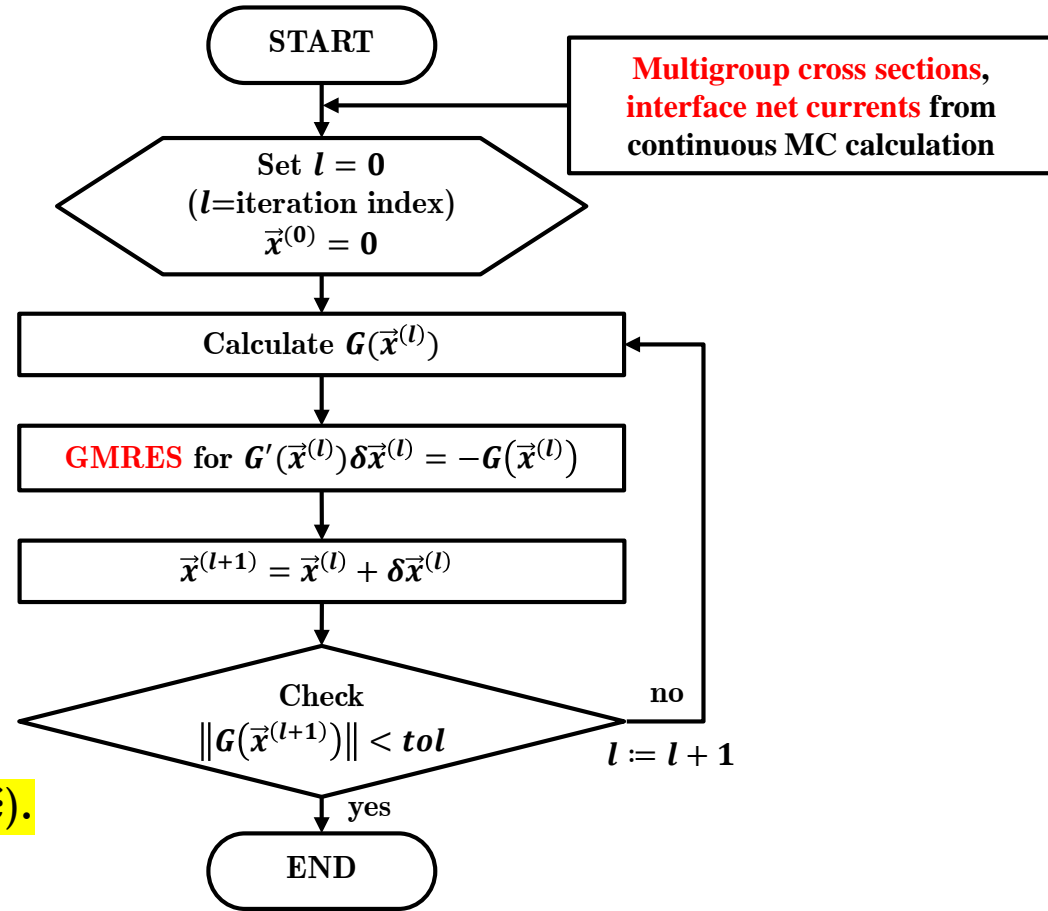


Fig. 4. PCDF Iteration with the JFNK method.

3. Numerical Results (1/11)

□ Pin Specifications

- Pin pitch = 1.26 cm
- Fuel radius = 0.4095 cm
- UO_2 : 10.2 g/cc with U-235 enrichment 3.3 w/o
- Moderator: 800 ppm boron concentration
- Divisions of surfaces for application of PCDFs

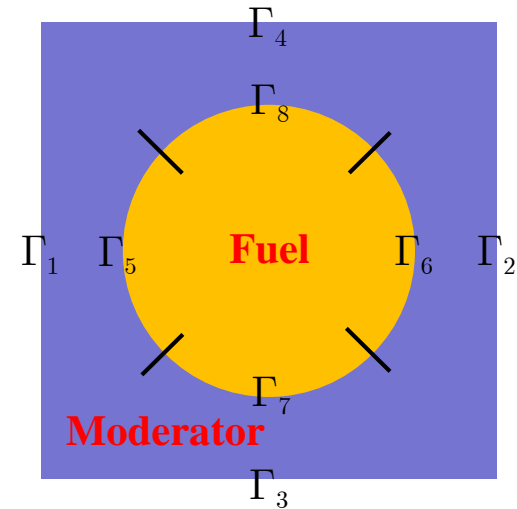


Fig. 5. 2-D UO_2 Pin Geometry.

□ Test of HIRE theory with PCDF iteration

Step 1. Continuous-energy MC calculations

Step 2. Generation of region-averaged multigroup XS and net currents on region interfaces

Step 3. PCDF iteration with multigroup method of characteristics (MOC) calculation

3. Numerical Results (2/11)

□ Test Problems

- Test Problem 1: **One** pin-cell problem (**reflective BC**)
- Test Problem 2: **One** pin-cell problem (**albedo BC**)
- Test Problem 3: **2 × 2** pin-cell problem (3 fuel pins and 1 moderator) (**reflective BC**)
- Test Problem 4: **4 × 4** pin-cell problem (fuel and **baffle**) (**albedo BC**)
- Test Problem 5: **One** pin-cell problem (**rim effect** in depletion)

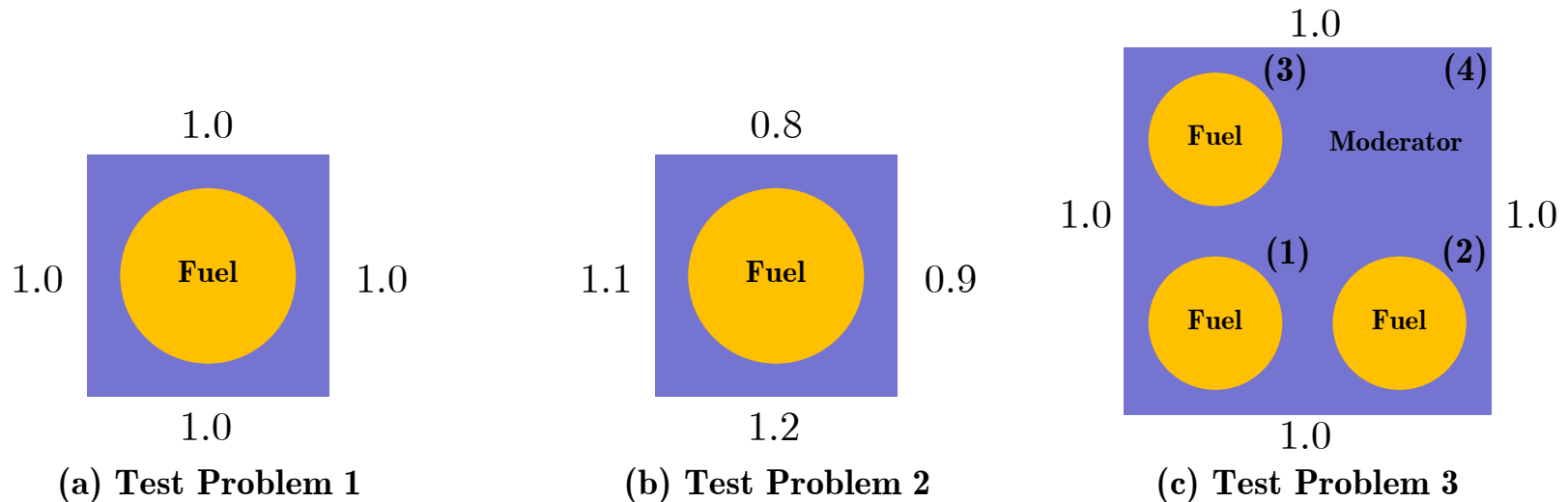


Fig. 6. Geometry of Test Problems 1~3
(#. # are albedo values at surfaces).

3. Numerical Results (3/11)

□ Computational Conditions

- Continuous-energy Monte Carlo calculation: **McBOX**
 - No. of inactive cycles: 100
 - No. of active cycles: 200
 - No. of histories per cycles: 5,000,000
 - Energy group boundary: 0.625 eV

- Two-group MOC calculation : **CRX3**
 - Mesh division: 4 rings with 8 sectors in a pin cell
 - Angular mesh: 8 azimuthal/3 polar angles per quadrant
 - No. of rays per cell per angle: 50
 - Stopping criteria: **1.0e-7** for fission source and k_{eff}

- PCDF iteration
 - Stopping criterion: **1.0e-7** for surface net current

3. Numerical Results (4/11)

□ Numerical Results: Two-Group Cross Sections

Table I. Two-group cross sections [cm^{-1}] for test problem 2

Region	Group	σ_t	$\nu\sigma_t$	$\sigma_{s0,*\rightarrow 1}$	$\sigma_{s0,*\rightarrow 2}$
Fuel	1	4.0702E-01	2.3291E-02	3.7740E-01	6.7072E-04
	2	7.6754E-01	6.9308E-01	4.0395E-04	3.9355E-01
Moderator	1	8.7733E-01	0.0000E+00	8.3570E-01	4.0810E-02
	2	1.9473E+00	0.0000E+00	4.6988E-04	1.9066E+00

- Group cross sections in Test Problem 1 and 3 are slightly different from those in Table I, even for the same material, due to the differing leakages.

3. Numerical Results (5/11)

□ Numerical Results: PCDFs

Table II. PCDFs for test problem 2

Group	f_1^-	f_2^-	f_3^-	f_4^-
1	0.99904	0.99768	0.99511	0.99184
2	0.99773	0.99808	0.99270	0.99015
Group	f_5^+	f_6^+	f_7^+	f_8^+
1	1.00576	1.00521	1.00606	1.00550
2	0.99630	0.99653	0.99405	0.99696
Group	f_5^-	f_6^-	f_7^-	f_8^-
1	0.99432	0.99388	0.99449	0.99288
2	1.00253	1.00289	1.00370	1.00282

- PCDF are not symmetric, because of the boundary conditions.

3. Numerical Results (6/11)

□ Numerical Results: Multiplication Factor

Table III. Multiplication factor from PCDF iteration

Problem	k_{eff}^{ref}	k_{eff}^{HIRE}	Δk_{eff} (pcm)	Number of fixed-point iterations /MOC calculations	Number of JFNK iterations /MOC calculations
1	1.283819 (± 2.6 pcm)*	1.283823	0.4	987/988	2/23
2	1.125992 (± 2.6 pcm)*	1.125990	-0.2	825/826	4/60
3	1.199928 (± 2.8 pcm)*	1.199925	-0.3	847/848	4/124

* Standard deviation of the reference MC calculation.

- Note that the multiplication factors of the PCDF iteration converge to those in the reference calculations for all three test problems.

3. Numerical Results (7/11)

□ Numerical Results: Flux Error

Table IV. Maximum relative error in region-averaged flux

Problem	Group 1 (%)	Std.* of Group 1 (%)	Group 2 (%)	Std.* of Group 2 (%)
1	2.64E-05	1.25E-03	1.33E-04	2.84E-03
2	7.63E-05	2.03E-03	1.07E-03	4.46E-03
3	5.82E-02	4.59E-03	1.63E-03	4.60E-03

*Std.: standard deviation of the region-averaged flux in the reference MC calculation

- Three test problems have maximum errors of less than 0.06%.
 - Hence, the converged PCDFs give accurate region-averaged fluxes in the multigroup transport calculation.
- Tables III and IV reveal that the HIRE theory generates group constants (cross sections and PCDFs) that can reproduce the multiplication factor and region-averaged reaction rates of the continuous-energy MC transport calculation.

3. Numerical Results (8/11)

- **Test Problem 5: Sub-pin level depletion (rim effect) (via MC code McBOX)**
- 10 equally spaced concentric rings in fuel region
 - Continuous-energy nuclear data library : ENDF/B-VII.0 at 600K
 - Decay constant and yield data : ORIGEN2 library
 - Matrix exponential calculation : Chebyshev rational approximation method (CRAM)
 - Power : 100 kW (520 full power days)

Table V. Materials and radii of concentric rings

Material Region Index	Radii of Concentric Rings [cm]	Material
1	0.03922	UO ₂
2	0.07844	UO ₂
3	0.11765	UO ₂
4	0.15687	UO ₂
5	0.19609	UO ₂
6	0.23531	UO ₂
7	0.27453	UO ₂
8	0.31374	UO ₂
9	0.35296	UO ₂
10	0.39218	UO ₂
11	0.40005	Helium
12	0.45720	Cladding
13	-	Moderator

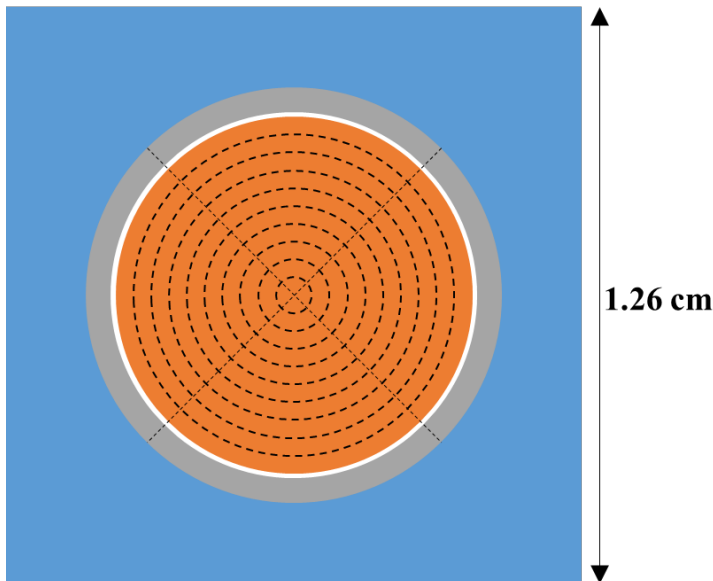


Fig. 7. UO₂ pin-cell problem; axial length with 100 cm (all reflective boundary conditions)

3. Numerical Results (9/11)

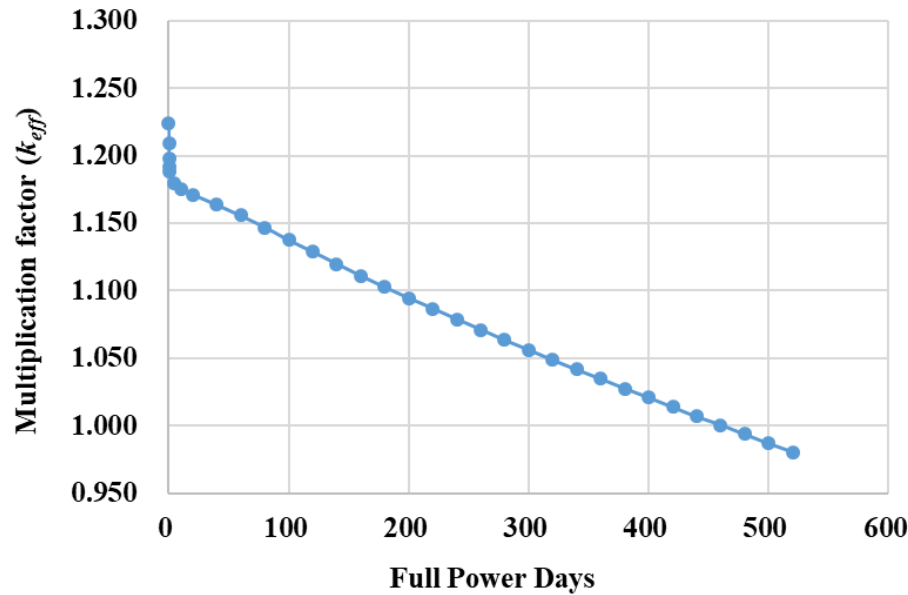


Fig. 8. Multiplication factors versus full power days.

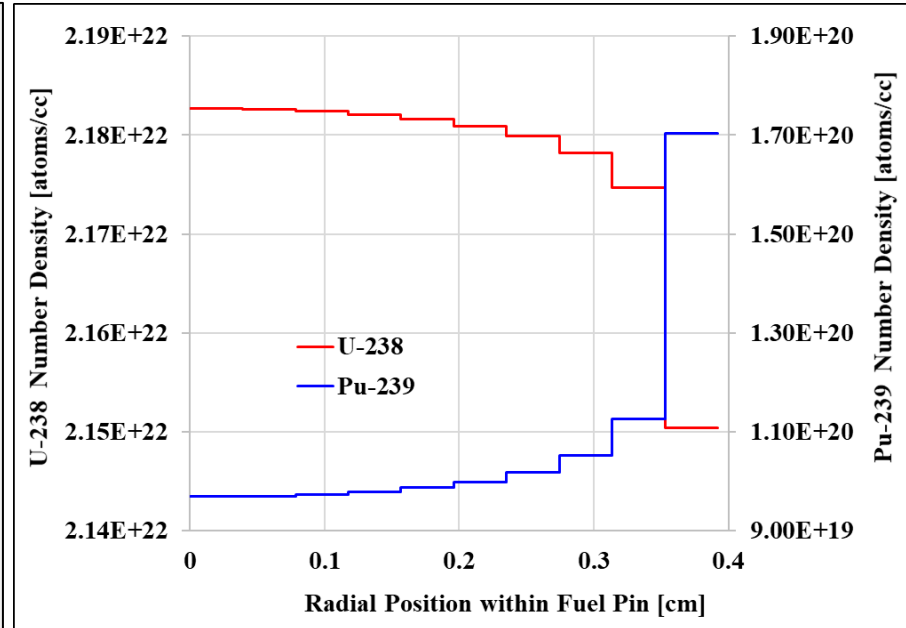


Fig. 9. Number densities of **U-238** (left y-axis) and **Pu-239** (right y-axis) versus radial position within the fuel pin at 520 full power days.

- **The rim effect** is observed in a **high burnup UO_2 fuel** (at 520 full power days).

3. Numerical Results (10/11)

□ Application of two-group HIRE theory to high burnup UO_2 fuel pin

- Continuous-energy MC simulation (McBOX) to tally two-group cross sections (collision estimator) and surface net currents (surface-crossing estimator)
 - No. of inactive cycles : 50
 - No. of active cycles : 200
 - No. of histories per cycles : 5,000,000
 - Energy group boundary : 1 eV
- Two-group MOC calculation for PCDF iteration (multigroup MOC code CRX3)
 - Mesh division : 13 rings with 8 azimuthal sectors in a pin cell
 - Angular mesh : 8 azimuthal/3 polar angles per quadrant
 - No. of ray per cell per angle: 150
 - Stopping criteria : $1.0\text{e-}8$ for fission source and k_{eff}
 - Stopping criterion for PCDF iteration : $1.0\text{e-}6$ for surface net current

Table VI. Multiplication factor from PCDF iteration with JFNK method

$k_{\text{eff}}^{\text{MC}}$	$k_{\text{eff}}^{\text{MOC}}$	Δk_{eff} (pcm)	Number of PCDF iterations	Number of MOC calculations	Computing times for PCDF iterations
0.980556 (2.2 pcm)*	0.980552	-0.434 pcm	3	146	8.42 sec**

*Standard deviation of the continuous-energy MC simulation

**Intel® Core™ i7-7700K processor

3. Numerical Results (11/11)

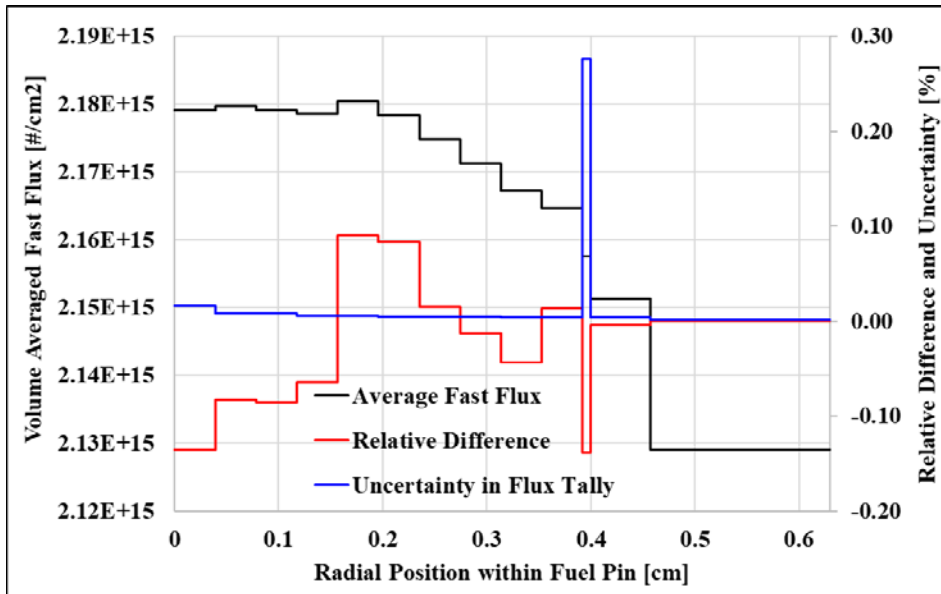


Fig. 10. Region-wise volume averaged fast scalar flux distributions (left axis), their **relative difference distributions** (right axis), and **uncertainty distributions in fast flux**(right axis).

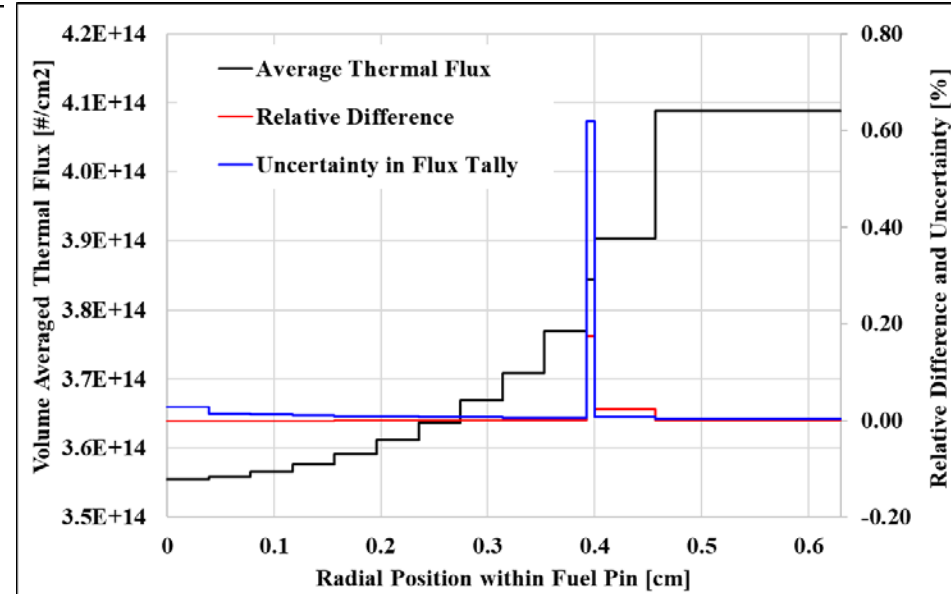


Fig. 11. Region-wise volume averaged thermal scalar flux distributions (left axis), their **relative difference distributions** (right axis), and **uncertainty distributions in thermal flux** (right axis).

- Relative differences in flux distributions less than 0.2%.
- Uncertainty errors in HIRE-theoretic group constants (cross sections and net currents)
 - Small fast net current (near to zero) at the innermost region
 - Inefficient collision estimator at helium gap

4. Summary and Concluding Remarks (1/2)

□ Summary

- Homogeneity and Isotropy Restoration (**HIRE**) theory:
 - Provides multigroup transport equations with
 - ✓ Material region-wise homogeneous XS (restoration of homogeneity)
 - ✓ Angle-independent total XS (restoration of isotropy)
 - ✓ In scattering terms, only σ_{s0} term remains in the multigroup transport equations.
 - Partial current discontinuity factors (**PCDFs**) are introduced to preserve the neutron leakages at material interfaces.
- For the test problems, HIRE theory with **PCDF iteration** via **JFNK** gives accurate results very fast, compared to the MC reference values:
 - Multiplication factor with errors < 1 pcm.
 - Region-averaged flux with errors $< 0.07\%$.

4. Summary and Concluding Remarks (2/2)

□ Concluding Remarks

- The volume of integration for material region can be chosen:
 - 1) A **multi-region** such as pin-cell homogenization or baffle-reflector homogenization
 - 2) **Resolved regions** such as rings in a fuel rod for
 - i) rim effect in depletion
 - ii) fuel temperature feedback effect

4. Summary and Concluding Remarks (2/2)

□ Concluding Remarks

- The volume of integration for material region can be chosen:
 - 1) A **multi-region** such as pin-cell homogenization or baffle-reflector homogenization
 - 2) **Resolved regions** such as rings in a fuel rod for
 - i) rim effect in depletion
 - ii) fuel temperature feedback effect
- Multigroup cross sections and PCDFs could be **tabulated** or **functionalized** in :
 - i) α values
 - ii) Burnup
 - iii) Fuel and moderator temperatures

4. Summary and Concluding Remarks (2/2)

□ Concluding Remarks

- The volume of integration for material region can be chosen:
 - 1) A **multi-region** such as pin-cell homogenization or baffle-reflector homogenization
 - 2) **Resolved regions** such as rings in a fuel rod for
 - i) rim effect in depletion
 - ii) fuel temperature feedback effect
- Multigroup cross sections and PCDFs could be **tabulated** or **functionalized** in :
 - i) α values
 - ii) Burnup
 - iii) Fuel and moderator temperatures
- Need a study for “representativeness” of a unit problem, depending on the reactor types: a **square pin cell**, a **super-hexagon of fuel assemblies**
- for the choice of few-group **G (2 – 10)**), depending on the reactor types.
- The few-group HIRE equations can be solved efficiently in **Two-Level p-CMFD** acceleration framework.

5. References

1. N. Z. Cho, Y.G. Jo, and S. Yuk, “A New Derivation of the Multigroup Transport Equations via Homogeneity and Isotropy Restoration Theory,” *Ann. Nucl. Energy*, **110**, 798-804 (2017).
2. Y.G. Jo, N. Z. Cho, and S. Yuk, “Depletion Rim Effect Incorporated in HIRE-Theoretic Multigroup Transport Equations,” *Trans. Am. Nucl. Soc.*, **117**, 1436-1439 (2017).
3. N. Z. Cho, “A Proposed New Framework for Nuclear Reactor Physics Analysis with Transport Calculation,” *Transactions of the Korean Nuclear Society Autumn Meeting*, Yeosu, Korea, October 24-26, 2018.
https://www.kns.org/files/pre_paper/40/18A-132조남진I.pdf
4. N. Z. Cho, “The Roles of Transport Partial Current Information in Two-Level p-CMFD Acceleration in the Whole-Core Transport Calculation,” *Trans. Am. Nucl. Soc.*, **121**, 1323-1326 (2019).
5. N. Z. Cho, “Krylov Subspace Wraps around the Two-Level p-CMFD Acceleration in the Whole-Core Transport Calculation,” *Trans. Am. Nucl. Soc.*, **123**, 1327-1330 (2020).

Thank you!